Updates to the NuMI Flux Simulation at MicroBooNE

Version 1.0

MicroBooNE Collaboration[*]

June 11, 2024

---

[*]microboone_info@fnal.gov

Contents

1   INTRODUCTION

The NuMI flux prediction [1] being used by all experiments at Fermilab that are sensitive to the NuMI beam is based on *Geant* v4.9.2.03 (G4.9) and uses the default *FTFP-BERT* physics list with no custom cross sections [2]. In order to correct these predictions to match world data, *PPFX,* the Package to Predict the FluX, is used to reweight the flux prediction. In kinematic regions of overlap between the prediction and data, mainly NA49 measurements are used to correct for various hadron production processes. Specifically, *PPFX* looks at the entire ancestry chain of the neutrino, up to the incident 120 GeV proton beam, and applies corrections for various hadron interactions based on said data. These corrections are implemented as a function of the Feynman-x (x_F) [3] and transverse momentum (p_T) of the incident hadron. More details about this can be found in Ref. [4].

Typically, the NuMI neutrino flux prediction is well constrained by the hadron production data on-axis. However, since MicroBooNE [5] lies far off-axis from the NuMI beam ($\sim 8°$), the flux is less covered by the available hadron production data. Moreover, the beamline geometry simulation failed to account for the presence of a row of steel shielding blocks (~ 40m in length) in the NuMI target hall directly above the beamline. The impact of this bug changes the flux at MicroBooNE by as much as $\sim 40\%$ in some regions, and is energy dependent.

To address these issues, we have overhauled the NuMI flux simulation by

- Adding the missing shielding blocks

- Updating the *Geant* version from v4.9.2 to v4.10.4 for the *FTFP-BERT* physics list

- Updating *PPFX* to account for this underlying model change

We note that efforts to move to *Geant* v4.10.4 had also been ongoing at the NOvA experiment, and related updates to the *PPFX* package were also being pursued by NOvA and *PPFX* developers. The combined effect of all the aforementioned changes are shown below in Figs 1 and 2. Figs 3 and 4 also show comparisons for the summed flux of neutrinos and anti-neutrinos. The correlation matrix representing the hadron production uncertainties in the new flux model based on updated *PPFX* is given below in Fig 5. Finally, Figs 9-Figs 12 in Appendix A show the breakdown of the updated *Geant* 4.10.4-based flux prediction for each parent type.
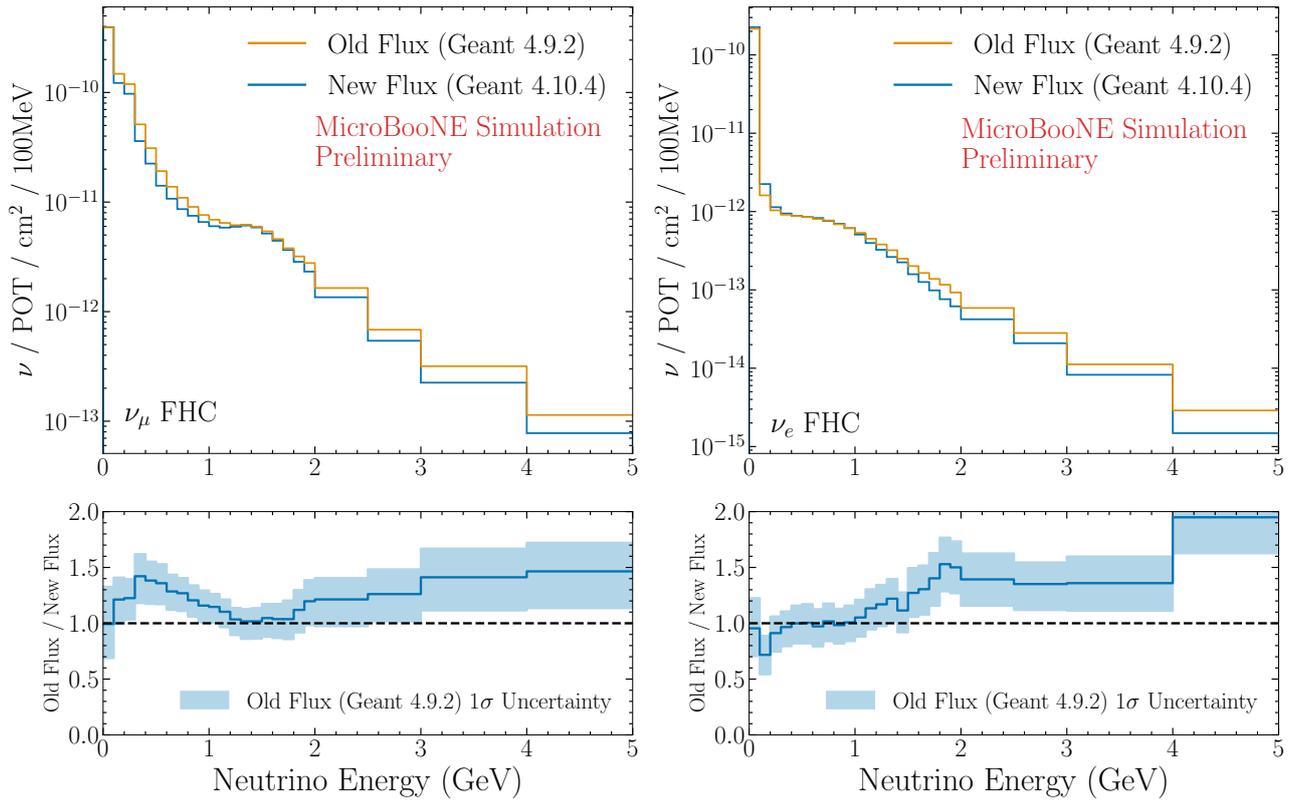
Figure 1: Comparison of the old flux model (*Geant 4.9.2*) before bug-fixes to the new flux model (*Geant 4.10.4*) with proper inclusion of the steel shielding blocks and updated cross-section and uncertainty treatment. The left (right) panel shows the ν_μ (ν_e) contribution for Forward Horn Current, or FHC. Ratios are taken with respect to the newer flux model (blue). Also shown are $\pm 1\sigma$ uncertainties of the older flux model to illustrate the change relative to the previous model's uncertainties.
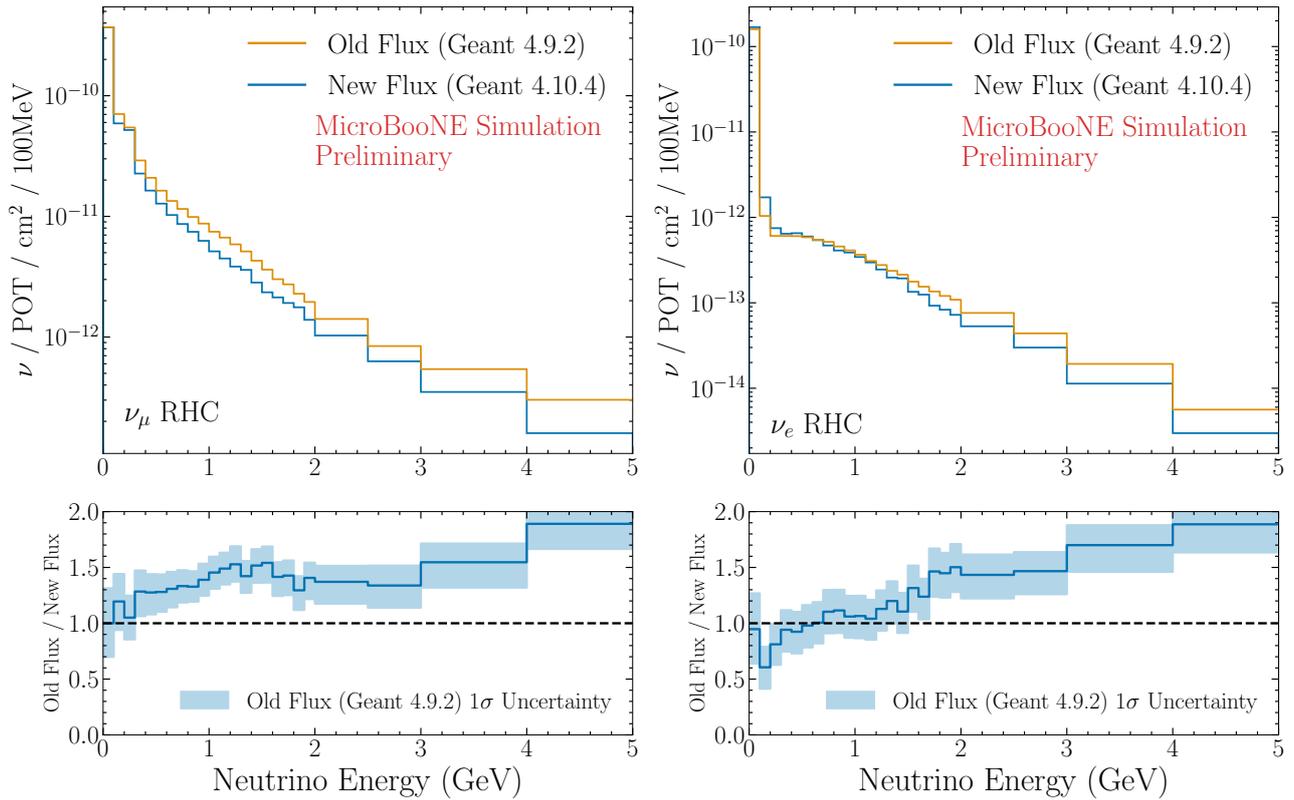
Figure 2: Similar to Fig.1 but for the Reverse Horn Current (RHC) NuMI configuration. Comparison of the old flux model (*Geant 4.9.2*) before bug-fixes to the new flux model (*Geant 4.10.4*) with proper inclusion of the steel shielding blocks and updated cross-section and uncertainty treatment. The left (right) panel shows the ν_μ (ν_e) RHC contribution. Ratios are taken with respect to the newer flux model (blue). Also shown are $\pm 1\sigma$ uncertainties of the older flux model to illustrate the change relative to the previous model's uncertainties.
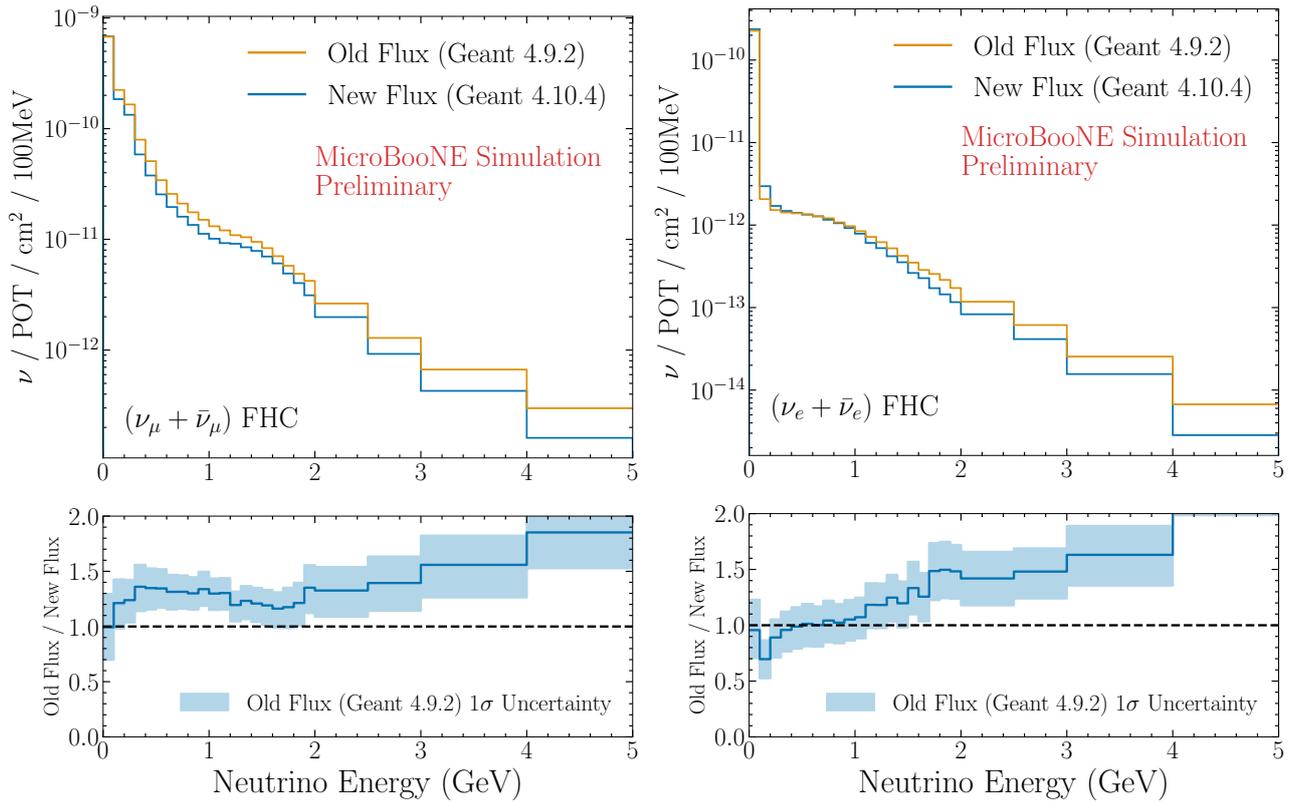
Figure 3: Comparison of the old flux model (*Geant 4.9.2*) before bug-fixes to the new flux model (*Geant 4.10.4*) with proper inclusion of the steel shielding blocks and updated cross-section and uncertainty treatment. The left (right) panel shows the FHC summed contribution from $\nu_\mu + \bar{\nu}_\mu$ ($\nu_e + \bar{\nu}_e$). Ratios are taken with respect to the newer flux model (blue). Also shown are $\pm 1\sigma$ uncertainties of the older flux model to illustrate the change relative to the previous model's uncertainties.
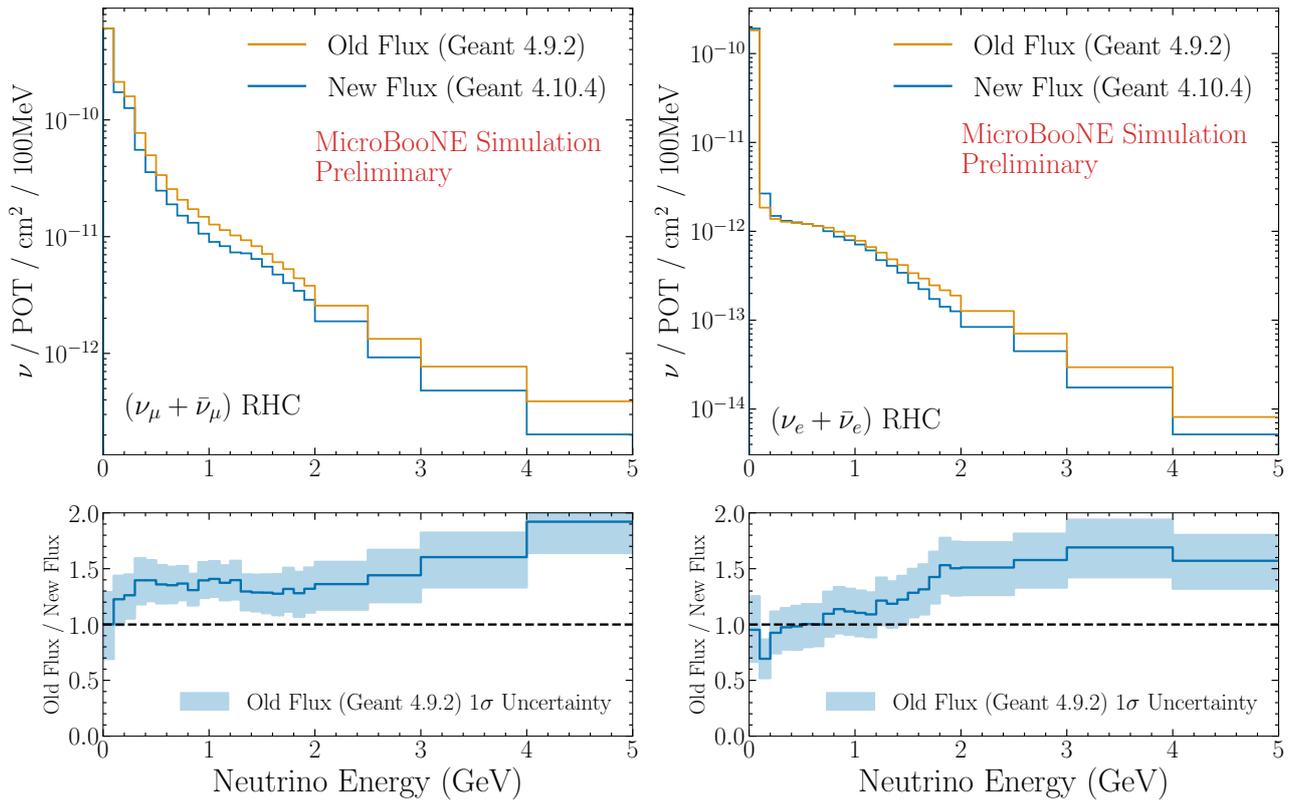
Figure 4: Similar to Fig.3 but for the Reverse Horn Current (RHC) NuMI configuration. Comparisons of the old flux model (*Geant 4.9.2*) before bug-fixes to the new flux model (*Geant 4.10.4*) with proper inclusion of the steel shielding blocks and updated cross-section and uncertainty treatment. The left (right) panel shows the RHC summed contribution from $\nu_\mu + \bar{\nu}_\mu$ ($\nu_e + \bar{\nu}_e$). Ratios are taken with respect to the newer flux model (blue). Also shown are $\pm 1\sigma$ uncertainties of the older flux model to illustrate the change relative to the previous model's uncertainties.
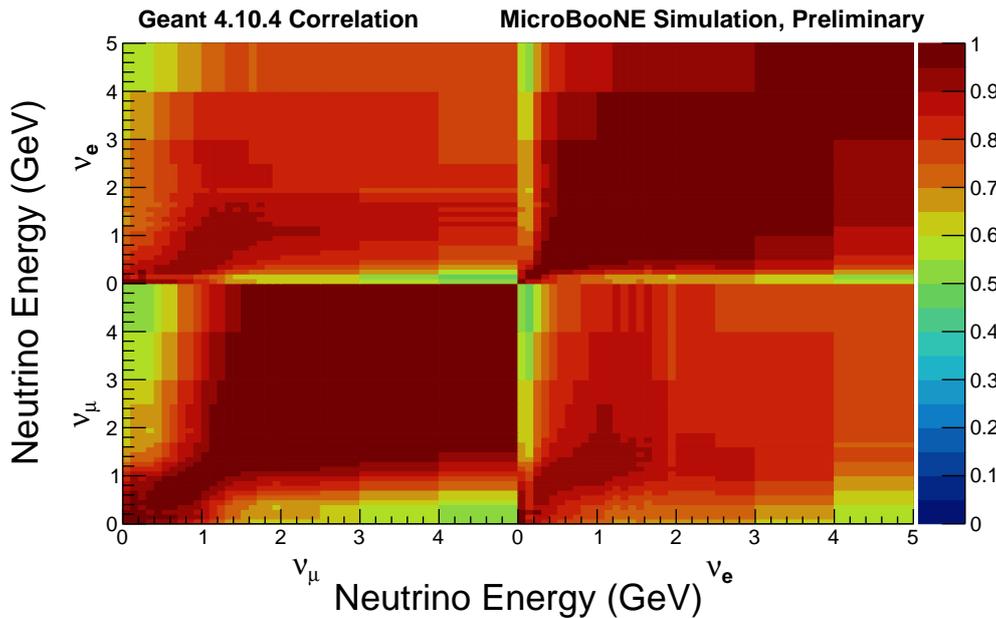
Figure 5: Correlation matrix between ν_μ and ν_e in true neutrino energy (between 0 and 5 GeV) for *Geant*4.10.4 model with updated PPFX and proper inclusion of the steel shielding blocks

2 GEANT 4.10.4

As mentioned previously, the weaker coverage of external hadron production data at 8° off-axis motivated the study into more modern *Geant4* versions for the underlying physics model in the flux simulation. The *FTFP-BERT* physics list in particular underwent substantial updates from *Geant* 4.9.2 and stabilized around 4.10.2-4.10.3 [6]. These updates included benchmarking of the underlying FTF string model to the relevant hadron production datasets from NA49 at 158 GeV [7] [8] and NA61 at 31 GeV [9]. This benchmarking includes tuning of relevant model parameters for string formation and fragmentation for high energy inelastic processes.

In particular, the modeling of kaon production, which is a dominant channel for the MicroBooNE flux, is much improved with this update. *Geant* 4.10.4 also includes a bug fix to the kaon re-interaction cross-section (which was first implemented in *Geant* 4.10.3*p*03, also see 2.2). Moreover, beyond *Geant* 4.10.4, the updates to the physics list do not show clear improvement with respect to external hadron production datasets. This is illustrated in figure 6 below for both π^+ and K^+ production at incident proton energies of 120 GeV. While 4.10.4 shows a marked improvement with respect to the older 4.9.2, especially in the K^+ production channel, the same cannot be said of 4.11.1. More details along with further comparisons are noted in [10].

(a) π^+ Production   **(b)** K^+ Production
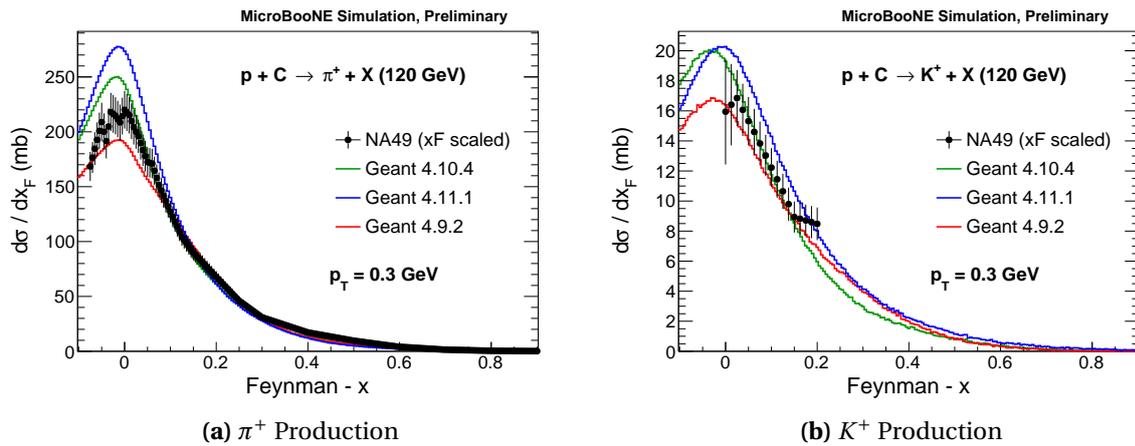
Figure 6: Comparison of production cross-sections for various *Geant* versions from existing 4.9.2 (red) to the chosen version 4.10.4 (green) along with version 4.11.1 (blue) with the NA49 measurement for the π^+ production channel (left) and K^+ production channel (right). The cross-sections are reported as a function of the Feynman-x observable. The NA49 reported cross-sections are also extrapolated from 158 GeV down to 120 GeV using FLUKA [11] account for the scaling violation, similar to the assumption in *PPFX*. However, the scaling violation from $158 \rightarrow 120$ GeV is fairly small ($\sim 2\%$)

Building on existing efforts by NOvA to update the *Geant* version, we have therefore fully updated our simulation to 4.10.4. This also ensures a more coherent development path for all experiments using the NuMI beamline.

2.1   Updating PPFX

Beyond the central value prediction, we've also updated the NuMI hadron production uncertainties to account for certain issues within PPFX

- First, we incorporate a bug-fix implemented by ICARUS in the calculation of x_F, involving interactions with an incident meson.

- We also implement additional uncertainties at negative Feynman-x ($x_F < 0$) for incident nucleons (either proton or neutron) that interact with non-Carbon nuclei within the beamline and aren't constrained by external hadron production data. These interactions previously were not assigned any uncertainties within the *PPFX* framework. This is an important category of interactions for the flux at MicroBooNE's off-axis angle. The uncertainties for such interactions are at the level of ~ 40% across bins of x_F.

PPFX has also been updated to handle the new *Geant* version, since it previously used cross-sections from 4.9.2 to derive the appropriate weights. The updates include recomputing cross-sections and yields for hadron production, involving ($\pi^\pm, K^\pm, K_L^0, p, n$) as well as the corrections for particle propagation along the target and the rest of the beamline geometry. The updates to PPFX were validated by checking the new flux prediction at an on-axis location. For an on-axis flux, the coverage of external hadron production data used within PPFX is very good, i.e. a large portion of the flux is constrained by NA49 and similar datasets. We therefore expect the updated flux prediction to be consistent with the previous flux prediction, after reweighting by PPFX. This is shown in Fig 7. The difference in integrated flux from $(2, 20)$ GeV going from the older *Geant4*-based model to the newer *Geant4*-based model is < 3%.
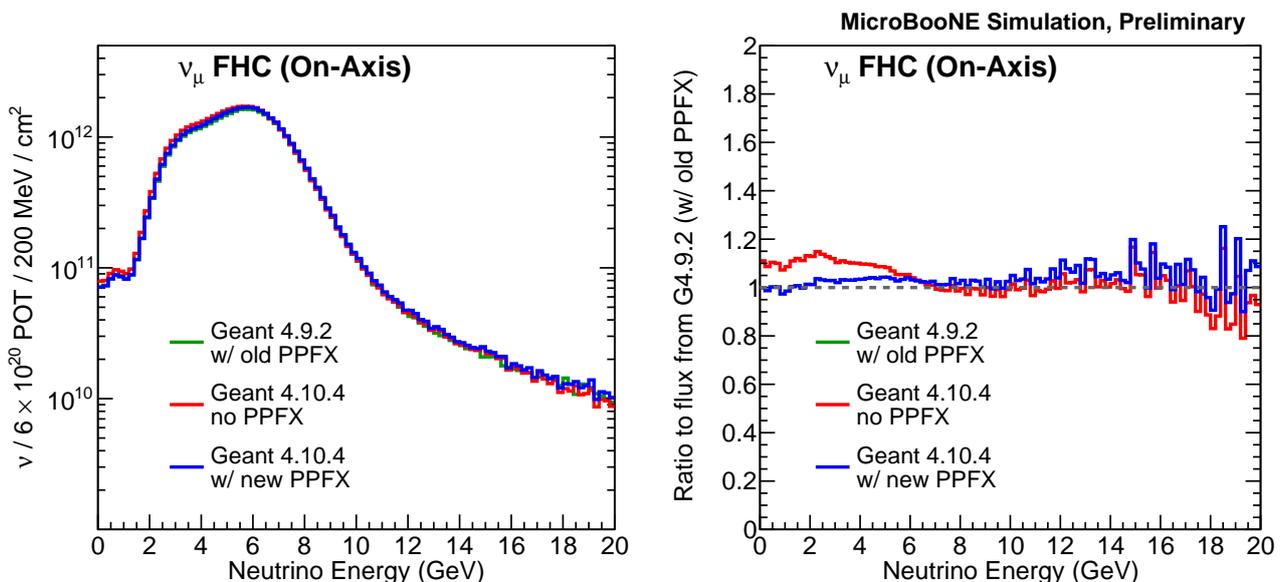
Figure 7: Comparison of the new flux model (*Geant 4.10.4*), including the shielding blocks and updated cross-sections and uncertainties, to the old flux model (*Geant 4.9.2*). The base *Geant 4.10.4* prediction without PPFX constraints are also shown in red. The ratios are taken with respect to the previous flux model.

2.2   BNB Validation

MicroBooNE's primary on-axis beam is called the Booster Neutrino Beam (BNB). It uses an incident proton beam at 8 GeV impinging on a beryllium target. Details of the BNB flux simulation are given in [12]. Although the flux simulation uses an older version, *Geant 4.8.1*, most of the cross sections used in the simulation of the beam are custom and therefore have a weaker dependence on the choice of *Geant* version. The BNB flux also applies constraints to hadron production from various external datasets, including for π^+ and K^+ production.

Nonetheless, similar to the previous validation, one can check the effect of updating the underlying *Geant* model to version 4.10.3p03. One of the notable features in the updated *Geant* version is a change from using Geisha routines to the Glauber-Gribov method for various re-interaction cross-sections. Version 4.10.3p03 also included a bug fix to the Glauber-Gribov calculation for inelastic kaon interactions [13]. The only part of the BNB flux simulation which is not custom is related to kaon interactions, both elastic and inelastic. Fig 8 shows that neither of these changes, i.e. with and without the kaon re-interaction bug-fix, or updating the *Geant4* version, have any impact on the flux prediction beyond $E_\nu > 0.2$ GeV and are well within existing flux uncertainties. Therefore, for the current MicroBooNE flux simulation, the existing BNB model is kept unchanged.

(a) ν_μ Flux   **(b)** ν_e Flux
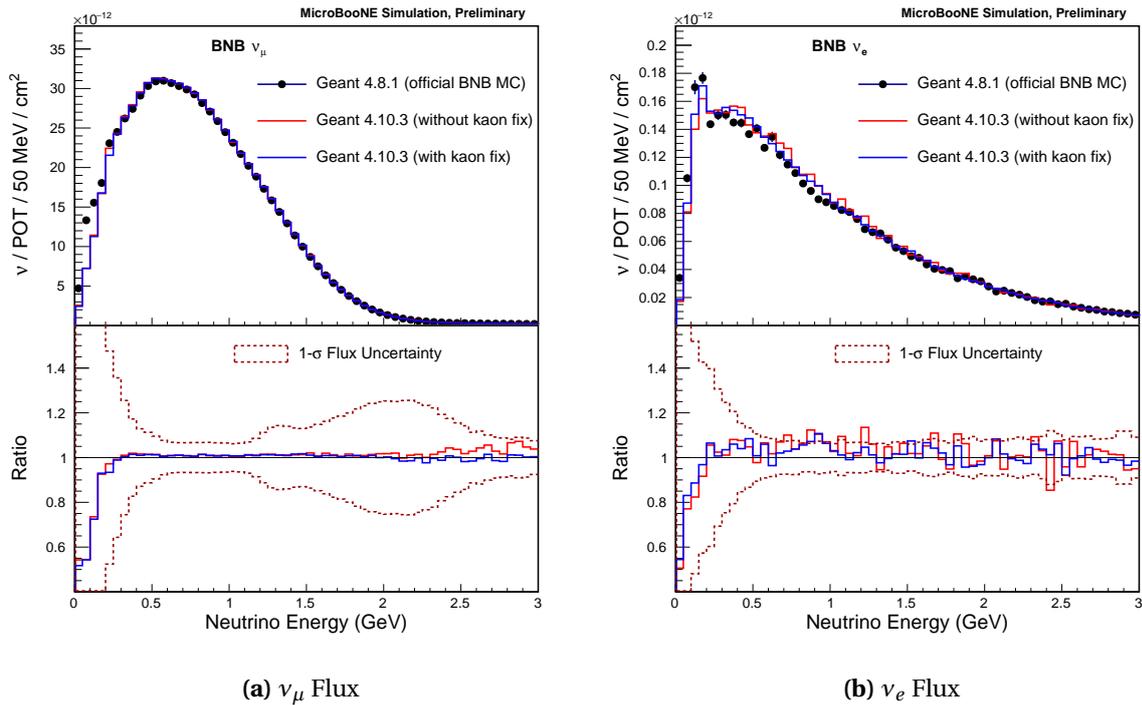
Figure 8: Comparison of various *Geant4* based flux predictions for the BNB with the markers representing existing BNB flux simulation based on version 4.8.1, red and blue representing the newer *Geant* version 4.10.3. Also shown are $\pm 1\sigma$ uncertainties from the 4.8.1-based flux model. Any changes to the BNB flux prediction due to different Geant versions are well within the assigned flux uncertainties. The MicroBooNE BNB flux simulation is kept unchanged from the 4.8.1-based model.

3 ACKNOWLEDGEMENTS

A NUMI FLUX BREAKDOWN

(a) ν_μ FHC

(b) ν_e FHC
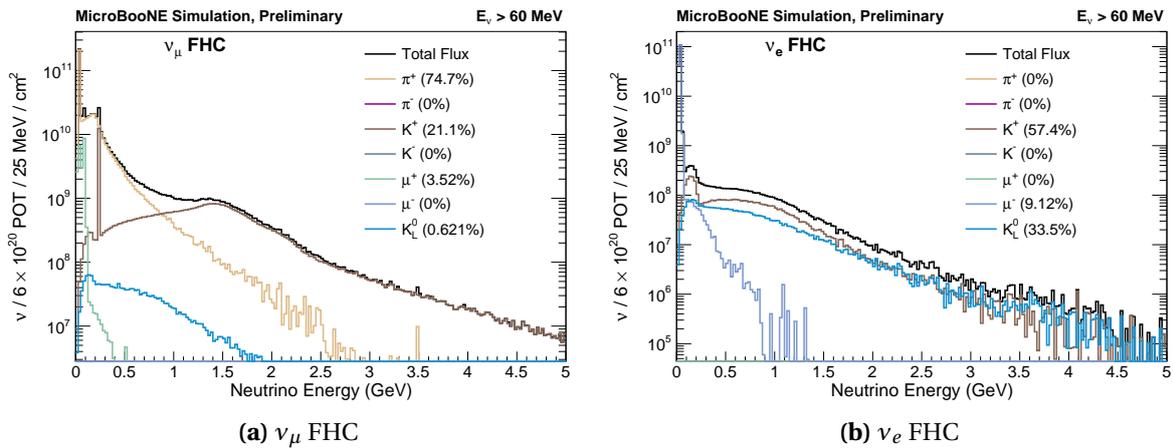
Figure 9: Updated *Geant* 4.10.4-based flux prediction for FHC, broken down by parent for ν_μ and ν_e. A 60 MeV threshold has been included in the percentages shown to avoid the flux from muon decay dominating these numbers.

(a) $\bar{\nu}_\mu$ FHC

(b) $\bar{\nu}_e$ FHC
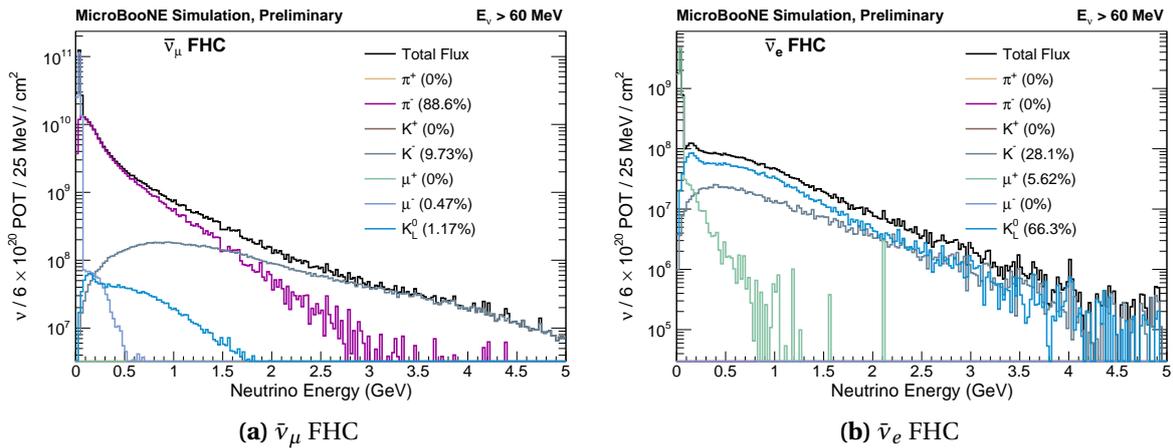
Figure 10: Updated *Geant* 4.10.4-based flux prediction for FHC, broken down by parent for $\bar{\nu}_\mu$ and $\bar{\nu}_e$. A 60 MeV threshold has been included in the percentages shown to avoid the flux from muon decay dominating these numbers.

(a) ν_μ RHC

(b) ν_e RHC
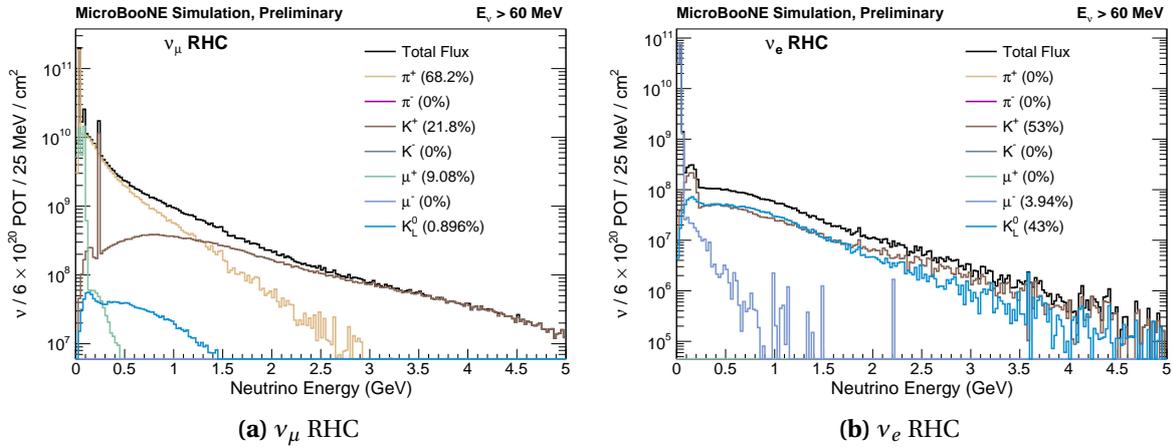
Figure 11: Updated *Geant* 4.10.4-based flux prediction for RHC, broken down by parent for ν_μ and ν_e. A 60 MeV threshold has been included in the percentages shown to avoid the flux from muon decay dominating these numbers.

(a) $\bar{\nu}_\mu$ RHC

(b) $\bar{\nu}_e$ RHC
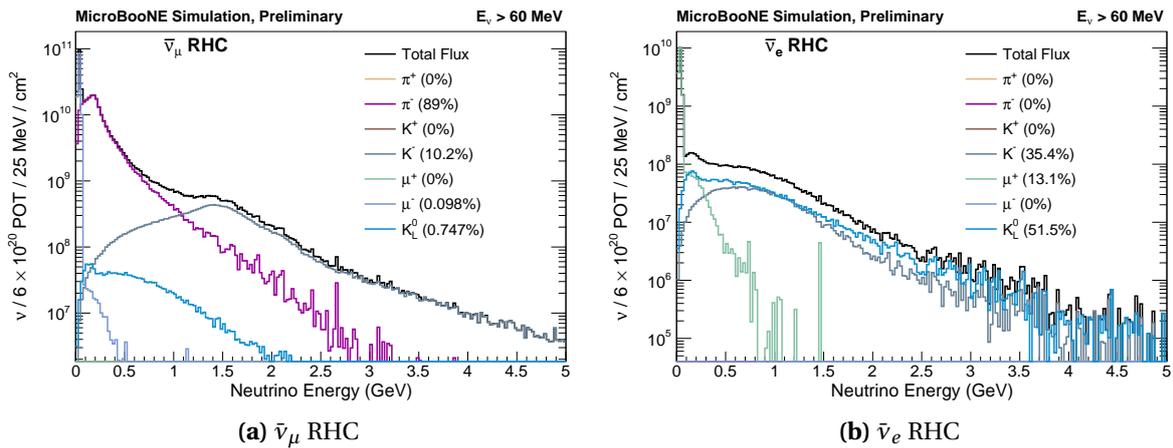
Figure 12: Updated *Geant* 4.10.4-based flux prediction for RHC, broken down by parent for $\bar{\nu}_\mu$ and $\bar{\nu}_e$. A 60 MeV threshold has been included in the percentages shown to avoid the flux from muon decay dominating these numbers.

REFERENCES

[1] P. Adamson et al. The NuMI Neutrino Beam. *Nucl. Instrum. Meth. A,* 806:279–306, 2016.

[2] S. Agostinelli et al. GEANT4–a simulation toolkit. *Nucl. Instrum. Meth. A,* 506:250–303, 2003.

[3] Richard P. Feynman. Very high-energy collisions of hadrons. *Phys. Rev. Lett.,* 23:1415–1417, 1969.

[4] L. Aliaga et al. Neutrino Flux Predictions for the NuMI Beam. *Phys. Rev. D,* 94(9):092005, 2016. [Addendum: Phys.Rev.D 95, 039903 (2017)].

[5] R. Acciarri et al. Design and Construction of the MicroBooNE Detector. *JINST,* 12(02):P02017, 2017.

[6] J. Yarba et al. Summary of Geant4 Hadronic Models Evolution from Release 9.6.p04 through 10.2.p02. https://cdcvs.fnal.gov/redmine/projects/g4/wiki/EvolutionHadModels-96-through-103b01.

[7] C. Alt et al. Inclusive production of charged pions in p+C collisions at 158-GeV/c beam momentum. *Eur. Phys. J. C,* 49:897–917, 2007.

[8] G. M. Tinti. Sterile neutrino oscillations in MINOS and hadron production in pC collisions, 2023. PhD Thesis, University of Oxford.

[9] N. Abgrall et al. Measurements of $\pi^{\pm}$, $K^{\pm}$, K_S^0, Λ and proton production in proton–carbon interactions at 31 GeV/c with the NA61/SHINE spectrometer at the CERN SPS. *Eur. Phys. J. C,* 76(2):84, 2016.

[10] J. Yarba et al. Geant4 Hadronic Models Evolution from Release 10.4.x onwards. https://cdcvs.fnal.gov/redmine/projects/g4/wiki/Evolution-Geant4-HadModels-from-104x.

[11] Alfredo Ferrari, Paola R. Sala, Alberto Fasso, and Johannes Ranft. FLUKA: A multi-particle transport code (Program version 2005). 10 2005.

[12] A. A. Aguilar-Arevalo et al. The Neutrino Flux Prediction at MiniBooNE. *Phys. Rev. D,* 79:072002, 2009.

[13] A. Higuera. Kaons in GEANT4. https://indico.fnal.gov/event/16852/contributions/40256/attachments/25010/31128/g4_higuera.pdf.